An Asymptotic Statistical Analysis of the Hyperanalytic Wavelet Transform

Ioana Firoiu, Corina Nafronita, IEEE Member, Dorina Isar, IEEE Member, Jean-Marc Boucher IEEE Senior Member and Alexandru Isar, IEEE Member
E-mail, ioana.firoiu@etc.upt.ro,corina.nafornita@etc.upt.ro, dorina.isar@etc.upt.ro, jm.boucher@telecom-bretagne.eu, alexandru.isar@etc.upt.ro

***Abstract*—We present an asymptotic statistical analysis of the Hyperanalytic Wavelet Transform (HWT) resulted after the estimation of their inter-scale and inter-band dependency. The resulting equations are useful for the design of different signal processing systems based on the wavelet theory used in communications.**

***Index Terms* — Asymptotic Analysis, Correlation, Hyperanalytic Wavelet Transform, Statistics.**

I. Introduction

A great number of Wavelet Transforms (WT) can be used to process images: denoising, compression, watermarking, to name only some applications which are useful in communications. The first one was the 2D Discrete WT, 2D DWT [1]. It has three main disadvantages, [2]: lack of shift invariance, lack of symmetry of the mother wavelets and poor directional selectivity. These disadvantages can be diminished using a complex wavelet transform [2, 3]. In the present paper we propose the utilization of a very simple implementation of the HWT, recently proposed, [4]. It has a high shift-invariance degree versus other quasi-shift-invariant WTs at same redundancy [4]. It has also an enhanced directional selectivity [4]. We have already applied it in denoising [5] and in watermarking [6] but we have not fully exploited yet its statistical properties. An appealing particularity of the HWT is the interscale dependency of the wavelet coefficients.

The structure of the paper is the following. In the second section, starting from the implementation of the 2D DWT, which second order statistical analysis was already reported [7], we describe a new implementation of the HWT. In the third section we present the results of the second order statistical analysis of the HWT. The fourth section concludes this paper.

II. HWT

Let us describe first the 2D DWT.

A. 2D DWT Implementation

The main advantage of the implementation of the 2D DWT described in the following is its flexibility, as it inherits some of the classes of mother wavelets developed in the framework of the 1D DWT, like the Daubechies, Symmlet or Coiflet families. Each of the iterations of the algorithm used for the computation of the 2D DWT implies several operations. First, the lines of the input image (obtained at the end of the previous iteration) are passed trough two different filters (a lowpass filter having the impulse response m_0 and a high-pass filter m_1) resulting two different sub-images. Then the lines of the two sub-images obtained at the output of the two filters are decimated with a factor of 2. Next, the columns of the two images obtained are low-pass filtered with m_0 and high-pass filtered with m_1. The columns of those four sub-images are also decimated with a factor of 2. Four new sub-images, representing the result of the current iteration (which corresponds to the current decomposition level (or scale)), are obtained. These sub-images are called subbands. The first sub-image, obtained after two lowpass filtering, is named approximation sub-image (or LL subband). The other three are named detail sub-images: LH, HL and HH. The LL sub-image represents the input for the next iteration. In the following, the coefficients of the DWT will be denoted with ${}_f D_m^k$, where f represents the image who's DWT is computed (considered as a bivariate random signal), m represents the current scale and k = 1 - for the subband LH, $k = 2$ - for HL, $k = 3$ - for HH and $k = 4$ - for LL. These coefficients are computed using the following relation:

$$ {}_f D_m^k [n_1, p_1] = \left\langle f(\tau_1, \tau_2), \psi_{m,n_1,p_1}^k (\tau_1, \tau_2) \right\rangle, \quad (1)$$

where the wavelets are real functions and can be factorized as:

$$ \psi_{m,n,p}^k (\tau_1, \tau_2) = \alpha_{m,n}^k (\tau_1) \cdot \beta_{m,p}^k (\tau_2), \quad (2)$$

and the two factors can be computed using the scale function $\varphi(\tau)$ and the mother wavelets $\psi(\tau)$ with the aid of the following relations:

$$ \alpha_{m,n}^k (\tau) = \begin{cases} \varphi_{m,n}(\tau), & k = 1, 4 \\ \psi_{m,n}(\tau), & k = 2, 3 \end{cases} \quad (3)$$

$$ \beta_{m,p}^k (\tau) = \begin{cases} \varphi_{m,p}(\tau), & k = 2, 4 \\ \psi_{m,p}(\tau), & k = 1, 3 \end{cases}, \quad (4)$$

where:

$$ \varphi_{m,n}(\tau) = 2^{-\frac{m}{2}} \varphi\left(2^{-m}\tau - n\right) \text{ and}$$

Manuscript received May 16, 2010. This work was supported by the Romanian Research Council under Grant no. 349/13.01.09 (sponsor and financial support acknowledgment goes here). Ioana Firoiu, Corina Nafronita, Dorina Isar and Alexandru Isar (phone 40 256 40 33 07, e-mail: alexandru.isar@etc.upt.ro) are with the "Politehnica" University TImisoara Romania and Jean Marc Boucher is with Telecom Bretagne, Brest, France (e-mail jm.boucher@telecom-bretagne.eu).

$$\psi_{m,n}(\tau) = 2^{-\frac{m}{2}}\psi\left(2^{-m}\tau - n\right). \quad (5)$$

Taking into account equations (3)-(5) it can be written:

$$\psi^k_{m,n,p}(\tau_1,\tau_2) = 2^{-m}\psi^k\left(2^{-m}\tau_1 - n, 2^{-m}\tau_2 - p\right), \quad (6)$$

where $\psi^k(\tau_1,\tau_2) = \psi^k{}_{0,0,0}(\tau_1,\tau_2)$.

B. Second Order Statistical Analysis of 2D DWT

We have proposed recently some results [7]. Let us recall in the following the most important ones.

The expectation of the wavelet coefficients equals zero:

$$\mu_{f D^k_m} = \begin{cases} 0, & k = 1,2,3 \\ 2^m \cdot \mu_f, & k = 4. \end{cases} \quad (7)$$

where μ_f represents the expectation of the input image.

The intercorrelation of two wavelet coefficients belonging to the subbands k_1 and k_2 and to the scales m_1 and $m_2 = m_1+q$ and having the geometrical coordinates (n_1, p_1) and (n_2, p_2) respectively, can be computed using the following relation:

$$\begin{aligned} &R_{D1D2}(m_1,m_2,k_1,k_2,n_1-n_2,p_1-p_2) = \\ &= \frac{1}{4\pi^2}\int_{-\infty}^{\infty}\int_{-\infty}^{\infty} S_f(\xi_1,\xi_2)\cdot 2^{2m_1}\cdot 2^q \cdot \\ &\exp\left(-j\cdot 2^{m_1}\left(\xi_1\left(2^q n_2 - n_1\right) + \xi_2\left(2^q p_2 - p_1\right)\right)\right)\cdot \\ &\cdot F\left\{\psi^{k_2}\right\}\left(2^{m_1}\cdot 2^q\xi_1, 2^{m_1}\cdot 2^q\xi_2\right)\cdot \\ &F^*\left\{\psi^{k_1}\right\}\left(2^{m_1}\cdot 2^q\xi_1, 2^{m_1}\cdot 2^q\xi_2\right)d\xi_1 d\xi_2 \end{aligned} \quad (8)$$

where we have denoted by $S_f(\xi_1,\xi_2)$ the power spectral density of the input image and by F the two-dimensional Fourier transform.

Manipulating this equation, we have proved in [7] that:

- the **inter-scale** ($q \neq 0$) **and inter-band** ($k_1 \neq k_2$) **dependency** of the wavelet coefficients depends on the autocorrelation of the input image, R_f and on the intercorrelation of the mother wavelets that generate the considered sub-bands, $R_{\psi^{k_2}\psi^{k_1}}$,

- For $k_1 = k_2 = k$, the intercorrelation of the wavelet coefficients expressed by (8) becomes an inter-scale and intra-band dependency. If the mother wavelet ψ^k generates by translations and dilations an **orthogonal** basis of $L^2(R)$ then the expression of the **inter-scale and intra-band dependency** becomes:

$$\begin{aligned} &R_{D1D2}(m_1,m_2,k_1,k_2,2^q n_1' - n_2, 2^q p_1' - p_2) = \\ &= 2^{2m_1+q} R_x\left(2^{m_1+q}(n_2 - n_1'), 2^{m_1+q}(p_2 - p_1')\right) \end{aligned} \quad (9)$$

If the input is a bi-dimensional i.i.d. white Gaussian noise with variance σ_w^2 and zero mean then *the wavelet coefficients with different resolutions are not correlated inside a sub-band*.

- For $m_1 = m_2 = m$ the intercorrelation of the wavelet coefficients expressed by (10) becomes an **intra-scale and intra-band dependency**:

$$\begin{aligned} &R_D(m,k,n_1' - n_2, p_1' - p_2) = \\ &= 2^{2m} R_x\left(2^m(n_2 - n_1'), 2^m(p_2 - p_1')\right). \end{aligned} \quad (10)$$

The last equation can be put in the equivalent form:

$$\begin{aligned} &R_D(m,k,n_1 - n_2, p_1 - p_2) = \\ &= \frac{1}{4\pi^2}\int_{-\infty}^{\infty}\int_{-\infty}^{\infty} S_f\left(2^{-m}\xi_1, 2^{-m}\xi_2\right)\cdot \\ &\cdot\exp\left(-j\left(\xi_1(n_2 - n_1) + \xi_2(p_2 - p_1)\right)\right)d\xi_1 d\xi_2 \end{aligned} \quad (11)$$

Taking in (11) the limit for $m \to \infty$, we obtain:

$$\begin{aligned} &R_D(\infty,k,n_1 - n_2, p_1 - p_2) = S_f(0,0)\cdot \\ &\cdot\delta[n_2 - n_1, p_2 - p_1]. \end{aligned} \quad (12)$$

We can affirm that asymptotically, the 2D DWT transforms every colored noise into a white one. Hence this transform can be regarded as a *whitening system in an intra-band and intra-scale scenario*.

A similar result can be obtained if the input is a bi-dimensional i.i.d. white Gaussian noise with variance σ_w^2 and mean zero, $f(\tau_1,\tau_2) = w(\tau_1,\tau_2)$. In this case relation (12) becomes:

$$R_{Dw}(n_1 - n_2, p_1 - p_2) = \sigma_w^2 \cdot \delta[n_2 - n_1, p_2 - p_1]. \quad (13)$$

We can state that, *in the same band and at the same scale, the 2D DWT does not correlate the i.i.d. white Gaussian noise*.

C. HWT Implementation

In the following we will use the definition of the analytic signal associated to a 2D real signal named hypercomplex signal. So, the hypercomplex mother wavelet associated to the real mother wavelet $\psi(x,y)$ is defined as:

$$\begin{aligned} &\psi_a(x,y) = \psi(x,y) + i\mathcal{H}_x\{\psi(x,y)\} + \\ &+ j\mathcal{H}_y\{\psi(x,y)\} + k\mathcal{H}_x\{\mathcal{H}_y\{\psi(x,y)\}\} \end{aligned} \quad (14)$$

where $i^2 = j^2 = -k^2 = -1$, *and* $ij = ji = k$, [8]. The values of the hypercomplex mother wavelets are quaternions. In function of the algebrical properties required, there are few definitions of quaternions. We adopted here the definition in [8] because it assures the comutativity of the quaternions product.

The HWT of the image $f(x,y)$ is:

$$HWT\{f(x,y)\} = \langle f(x,y), \psi_a(x,y)\rangle. \quad (15)$$

Taking into account relation (2) it can be written the equation (16). **So, the HWT of the image $f(x,y)$ can be computed with the aid of the 2D-DWT of its associated hypercomplex image.** This property permits the heritage of any mother wavelets from 2D DWT for HWT. In this respect the proposed variant of HWT differs of other variants of hyperanalytic wavelet transform, like for example that proposed in [9] which request special mother wavelets (like for example the elements of the Morse family of mother wavelets). The new HWT implementation, [4], presented in figure 1, uses four trees, each one implementing a 2D-DWT.

The first tree is applied to the input image. The second and the third trees are applied to 1D discrete Hilbert transforms computed across the lines ($\mathcal{H}_x$) or columns ($\mathcal{H}_y$) of the input image. The fourth tree is applied to the result obtained after the computation of the two 1D discrete Hilbert transforms of the input image.

$$\begin{aligned} &HWT\{f(x,y)\} = DWT\{f(x,y)\} + \\ &iDWT\left\{\mathcal{H}_x\{f(x,y)\}\right\} + jDWT\left\{\mathcal{H}_y\{f(x,y)\}\right\} + \\ &+kDWT\left\{\mathcal{H}_y\left\{\mathcal{H}_x\{f(x,y)\}\right\}\right\} = \\ &\left\langle f_a(x,y), \psi(x,y)\right\rangle = DWT\left\{f_a(x,y)\right\}. \end{aligned} \tag{16}$$

These are the so called initial computations. To obtain an enhanced directional selectivity some additional linear operations, represented in the right part of figure 1, must be performed [4]. The result is composed by two sequences of complex coefficients:

$$\begin{aligned} &z_+ = z_{+r} + jz_{+i} = \\ &= \left({}_f D^{1,2,3} - {}_{\mathcal{H}_y\{\mathcal{H}_x\{f\}\}} D^{1,2,3}\right) + \\ &+ j\left({}_{\mathcal{H}_x} D^{1,2,3} + {}_{\mathcal{H}_y} D^{1,2,3}\right) \end{aligned} \tag{17}$$

containing three subbands with positive angle direction orientations $\text{atan}(1/2)$, $\pi/4$ and $\text{atan}(2)$ and:

$$\begin{aligned} &z_- = z_{-r} + jz_{-i} = \\ &= \left({}_f D^{1,2,3} + {}_{\mathcal{H}_y\{\mathcal{H}_x\{f\}\}} D^{1,2,3}\right) + \\ &+ j\left({}_{\mathcal{H}_x} D^{1,2,3} - {}_{\mathcal{H}_y} D^{1,2,3}\right) \end{aligned} \tag{18}$$

containing three subbands with negative angle direction orientations -atan$(1/2)$, $-\pi/4$ and -atan(2). The principal advantage of the proposed implementation of HWT is that this complex transform is reduced at the 2D DWT permitting the heritage of some classes of mother wavelets, like the Daubechies, Symmlet or Coiflet families. This is why this implementation is adequate to a multi-wavelet environment.

III. HWT Statistical Analysis

Let us begin with the computation of the expectation of the coefficients z_+ and z_-:

$$\begin{aligned} &E\{z_+\} = E\left\{{}_f D^{1,2,3}\right\} - E\left\{{}_{\mathcal{H}\hat{y}\{\mathcal{H}\hat{x}\{f\}\}} D^{1,2,3}\right\} + \\ &jE\left\{{}_{\mathcal{H}\hat{x}} D^{1,2,3}\right\} + jE\left\{{}_{\mathcal{H}\hat{y}} D^{1,2,3}\right\} = 0 \end{aligned} \tag{19}$$

because all the four terms of the right hand side equal zero, representing expectations of detail coefficients of 2D DWTs (see equation (7)). Using similar arguments it can be proved that $E\{z_-\} = 0$. In the following is computed the intercorrelation between the real and imaginary parts of the coefficients z_+ and z_-. For the coefficients z_+ we obtain the

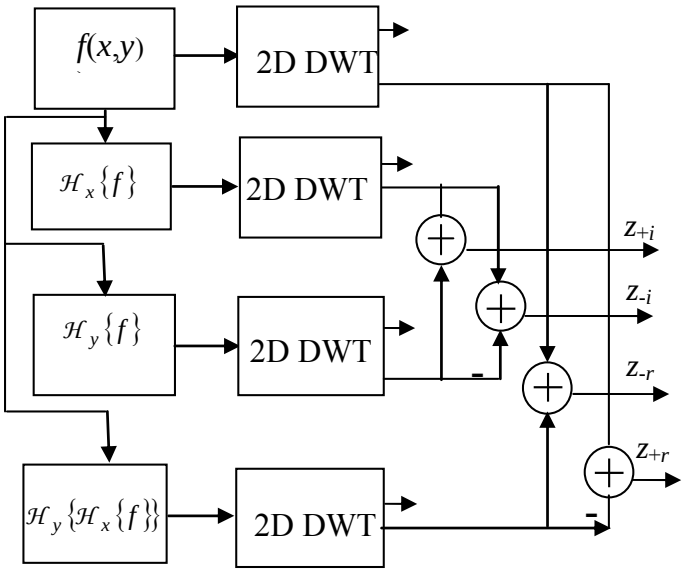

Fig. 1. The new HWT implementation architecture.

equation (20).

$$\begin{aligned} &R_{z_{+r}z_{+i}}[m_1,m_2,k_1,k_2,n_1,n_2,p_1,p_2] = \\ &= R_{DfD\mathcal{H}\hat{x}}(m_1,m_2,k_1,k_2,n_1-n_2,p_1-p_2) - \\ &-R_{D\mathcal{H}\hat{y}\{\mathcal{H}\hat{x}\}D\mathcal{H}\hat{x}}(m_1,m_2,k_1,k_2,n_1-n_2,p_1-p_2) + \\ &+R_{Df D\mathcal{H}\hat{y}}(m_1,m_2,k_1,k_2,n_1-n_2,p_1-p_2) - \\ &-R_{D\mathcal{H}\hat{y}\{\mathcal{H}\hat{x}\}D\mathcal{H}\hat{y}}(m_1,m_2,k_1,k_2,n_1-n_2,p_1-p_2). \end{aligned} \tag{20}$$

Each of the four terms from the right hand side can be expressed using equation (8) because they represent correlations of 2D DWT coefficients. The first factor of the expression under integral in the right hand side of equation (8) must be replaced by the interspectrum $S_{f\mathcal{H}\hat{x}\{f\}}$ to obtain the first term in the right hand side of equation (20) by the interspectrum $S_{\mathcal{H}\hat{y}\{\mathcal{H}\hat{x}\{f\}\}\mathcal{H}\hat{x}\{f\}}$ to obtain the second term, by the interspectrum $S_{f\mathcal{H}\hat{y}\{f\}}$ to obtain the third term and by the interspectrum $S_{\mathcal{H}\hat{y}\{\mathcal{H}\hat{x}\{f\}\}\mathcal{H}\hat{y}\{f\}}$ to obtain the last term of the right hand side of equation (20). These inter spectra can be expressed with the aid of the input power spectral density:

$$\begin{aligned} &S_{f\mathcal{H}\hat{x}\{f\}}(\xi_1,\xi_2) = j\,\text{sgn}\,\xi_1 S_f(\xi_1,\xi_2), \\ &S_{\mathcal{H}\hat{y}\{\mathcal{H}\hat{x}\{f\}\}\mathcal{H}\hat{x}\{f\}}(\xi_1,\xi_2) = -j\,\text{sgn}^2\,\xi_1\,\text{sgn}\,\xi_2 S_f \\ &S_{f\mathcal{H}\hat{y}\{f\}}(\xi_1,\xi_2) = j\,\text{sgn}\,\xi_2 S_f(\xi_1,\xi_2), \\ &S_{\mathcal{H}\hat{y}\{\mathcal{H}\hat{x}\{f\}\}\mathcal{H}\hat{y}\{f\}}(\xi_1,\xi_2) = -j\,\text{sgn}\,\xi_1\,\text{sgn}^2\,\xi_2 S_f. \end{aligned} \tag{21}$$

Using (8), (20) and (21), we obtain the equation (22). A similar expression can be deduced for the intercorrelation of the real and imaginary parts of the coefficients z_- and is given

in equation (23). Taking the limit for $m_1 \to \infty$, we obtain the equation (24) because $\operatorname{sgn}(0)=0$. Hence the real and imaginary parts of the coefficients z_+ and z_- are asymptotically decorrelated in a inter band context.

$$\begin{aligned}
&R_{z_{+r}z_{+i}}[m_1,m_2,k_1,k_2,n_1,n_2,p_1,p_2]=\\
&\frac{j}{4\pi^2}\int_{-\infty}^{\infty}\int_{-\infty}^{\infty}\Big[\operatorname{sgn}\left(2^{-m_1}2^{-q}\nu_1\right)+\operatorname{sgn}^2\left(2^{-m_1}2^{-q}\nu_1\right)\\
&\cdot\operatorname{sgn}\left(2^{-m_1}2^{-q}\nu_2\right)+\operatorname{sgn}\left(2^{-m_1}2^{-q}\nu_2\right)+\\
&+\operatorname{sgn}\left(2^{-m_1}2^{-q}\nu_1\right)\cdot\operatorname{sgn}^2\left(2^{-m_1}2^{-q}\nu_2\right)\Big]\cdot\\
&2^{-q}\cdot e^{-j\left(\nu_1\left(n_2-2^{-q}n_1\right)+\nu_2\left(p_2-2^{-q}p_1\right)\right)}\cdot\\
&\cdot\mathcal{F}\left\{\psi^{k_2}\right\}(\nu_1,\nu_2)\cdot\mathcal{F}^*\left\{\psi^{k_1}\right\}(\nu_1,\nu_2)\,d\nu_1 d\nu_2
\end{aligned}\tag{22}$$

$$\begin{aligned}
&R_{z_{-r}z_{-i}}[m_1,m_2,k_1,k_2,n_1,n_2,p_1,p_2]=\\
&\frac{j}{4\pi^2}\int_{-\infty}^{\infty}\int_{-\infty}^{\infty}\Big[\operatorname{sgn}\left(2^{-m_1}2^{-q}\nu_1\right)-\operatorname{sgn}^2\left(2^{-m_1}2^{-q}\nu_1\right)\\
&\cdot\operatorname{sgn}\left(2^{-m_1}2^{-q}\nu_2\right)-\operatorname{sgn}\left(2^{-m_1}2^{-q}\nu_2\right)+\\
&+\operatorname{sgn}\left(2^{-m_1}2^{-q}\nu_1\right)\cdot\operatorname{sgn}^2\left(2^{-m_1}2^{-q}\nu_2\right)\Big]\cdot\\
&2^{-q}\cdot e^{-j\left(\nu_1\left(n_2-2^{-q}n_1\right)+\nu_2\left(p_2-2^{-q}p_1\right)\right)}\cdot\\
&\cdot\mathcal{F}\left\{\psi^{k_2}\right\}(\nu_1,\nu_2)\cdot\mathcal{F}^*\left\{\psi^{k_1}\right\}(\nu_1,\nu_2)\,d\nu_1 d\nu_2
\end{aligned}\tag{23}$$

$$\begin{aligned}
&\lim_{m_1\to\infty}R_{z_{+r}z_{+i}}[m_1,m_2,k_1,k_2,n_1,n_2,p_1,p_2]=\\
&\lim_{m_1\to\infty}R_{z_{-r}z_{-i}}[m_1,m_2,k_1,k_2,n_1,n_2,p_1,p_2]=\\
&=0
\end{aligned}\tag{24}$$

In the following is identified the inter-band and the inter-scale dependencies of the real parts and respectively of the imaginary parts of the coefficients z_+ and z_-. Let us begin with:

$$\begin{aligned}
&R_{z_{+i}z_{+i}}[m_1,m_2,k_1,k_2,n_1,n_2,p_1,p_2]=\\
&=R_{D\mathcal{H}kD\mathcal{H}k}(m_1,m_2,k_1,k_2,n_1-n_2,p_1-p_2)+\\
&+R_{D\mathcal{H}kD\mathcal{H}y}(m_1,m_2,k_1,k_2,n_1-n_2,p_1-p_2)+\\
&+R_{D\mathcal{H}yD\mathcal{H}k}(m_1,m_2,k_1,k_2,n_1-n_2,p_1-p_2)+\\
&R_{D\mathcal{H}yD\mathcal{H}y}(m_1,m_2,k_1,k_2,n_1-n_2,p_1-p_2).
\end{aligned}\tag{25}$$

Each of the four terms from the right hand side can be expressed using equation (8) because they represent correlations of 2D DWT coefficients. The first factor of the expression under integral in the right hand side of equation (8) must be replaced by the power spectral density $S_{\mathcal{H}k}$ to obtain the first term in the right hand side of equation (25), by the interspectrum $S_{\mathcal{H}k\mathcal{H}y}$ to obtain the second term, by the interspectrum $S_{\mathcal{H}y\mathcal{H}k}$ to obtain the third term and by the power spectral density $S_{\mathcal{H}y}$ to obtain the last term of the right hand side of equation (25). These inter spectra can be expressed with the aid of the power spectral density of the input image and finally the equation (26) is obtained. Similar relations can be proved for the other orientations and for the real parts of the coefficients z_+ and z_-.

$$\begin{aligned}
&R_{z_{+i}z_{+i}}[m_1,m_2,k_1,k_2,n_1,n_2,p_1,p_2]=\\
&\frac{1}{4\pi^2}\int_{-\infty}^{\infty}\int_{-\infty}^{\infty}\Big[\operatorname{sgn}^2\left(2^{-m_1}2^{-q}\nu_1\right)+2\operatorname{sgn}\left(2^{-m_1}2^{-q}\nu_1\right)\\
&\cdot\operatorname{sgn}\left(2^{-m_1}2^{-q}\nu_2\right)+\operatorname{sgn}^2\left(2^{-m_1}2^{-q}\nu_2\right)\Big]\cdot\\
&2^{-q}\cdot e^{-j\left(\nu_1\left(n_2-2^{-q}n_1\right)+\nu_2\left(p_2-2^{-q}p_1\right)\right)}\cdot\\
&\cdot\mathcal{F}\left\{\psi^{k_2}\right\}(\nu_1,\nu_2)\cdot\mathcal{F}^*\left\{\psi^{k_1}\right\}(\nu_1,\nu_2)\,d\nu_1 d\nu_2
\end{aligned}\tag{26}$$

Taking the limit for $m_1 \to \infty$ in each such relation it results that those coefficients are asymptotically decorrelated.

IV. Conclusion

The HWT coefficients have strong inter-scale and inter-band dependencies. The inter-scale dependence is similar with the inter-scale dependence of the 2D DWT coefficients. The inter-band dependence is more complicated because the HWT has an increased number of subbands. Despite this additional complexity, we have proved that asymptotically the HWT coefficients are decorrelated like the 2D DWT coefficients. But the HWT has better translation invariance and better directional selectivity than the 2D DWT [4]. For these reasons we recommend the proposed variant of HWT for communications applications. The purpose of this paper was limited to the asymptotic analysis of the statistical comportment of the HWT coefficients. In the future we will find non asymptotic results as well and we will analyze the other dependencies: intra-band and inter-scale, inter-band and intra-scale and intra-band and intra-scale of HWT coefficients. Next, we will apply these results in image denoising and in watermarking.

References

[1] Stéphan Mallat, A wavelet tour of signal processing, Second edition, Academic Press, 1999.

[2] N. Kingsbury, Complex Wavelets for Shift Invariant Analysis and Filtering of Signals, *Applied and Comp. Harm. Anal.* 10, 2001, 234-253.

[3] N G Kingsbury, A Dual-Tree Complex Wavelet Transform with improved orthogonality and symmetry properties, *Proc. IEEE Conf. on Image Processing*, Vancouver, September 11-13, 2000, paper 1429.

[4] I. Adam, C. Nafornita, J-M Boucher and A. Isar, "A New Implementation of the Hyperanalytic Wavelet Transform", Proc. of IEEE Sympo. *ISSCS 2007*, Iasi, Romania, 401-404.

[5] Firoiu I., Nafornita C., Boucher J. –M., Isar A., Image Denoising Using a New Implementation of the Hyperanalytic Wavelet Transform, IEEE Transactions on Instrumentation and Measurements, vol. 58, Issue 8, August 2009, pp. 2410-2416,

[6] Corina Nafornita, Ioana Firoiu, Jean-Marc Boucher, Alexandru Isar, A new watermarking method based on the use of the hyperanalytic wavelet transform, Proc. SPIE Europe: Photonics Europe, Vol. 7000: Optical and Digital Image Processing, 70000W (Apr. 25, 2008), Strasbourg, France,

[7] C. Nafornita, I. Firoiu, D. Isar, J.-M. Boucher, A. Isar, "A Second Order Statistical Analysis of the 2D DWT", Proc. of IEEE Conference Communications 2010, Bucharest, Romania, June 2010,

[8] C. Davenport, Commutative Hypercomplex Mathematics, http://home.comcast.net/~cmdaven/nhyprcpx.htm

[9] S. Olhede and G. Metikas, The Hyperanalytic Wavelet Transform, Statistics section technical report TR-06-02, available at: http://arxiv.org/abs/math.ST/0605623.